Dispersive EM propagation through a thin waveguide

Luis A. Peche[1], Jandyr M. Travassos[1], 1-Coordenação de Geofísica, Observatório Nacional.

Abstract

It is know that surface layers may act as waveguides to the propagation of EM energy. Here we analyze the case where a concrete pavement can act as such when overlying a higher permittivity soil. We use the phase velocity spectra of the superficial wave propagation obtained from CMP data to invert for the waveguide refraction index and thickness, in a similar manner it is done when analyzing the dispersion of Rayleigh waves on multi-channel seismic data. Inversion is carried out using a minimization strategy that seeks models where the numerical dispersion curve matches the picked dispersion curve.

Introduction

Dispersive wave propagation may occur in the uppermost layer if its thickness is comparable to or smaller than the wavelength, and its lower boundary is a strong reflector. In this case EM waves will be trapped in the waveguide, traveling in a modal fashion (Annan et al., 1975). As in all cases the waveguide is overlain by air either the substratum has a lower or a significantly higher permittivity than the waveguide's (Arcone et al., 2003; van der Kruk et al., 2006). A low-velocity layer of wet soil over a higher velocity layer of sand and gravel is a studied example of the first case (Arcone et al., 2003; van der Kruk et al., 2006). An ice layer over water is an example of the second case (e.g., van der Kruk et al., 2007).

This paper deals with the case where the underlying layer has a higher permittivity, enough to provide strong enough reflection. In this case some energy leaks downwards and is quickly absorbed by a high-loss substratum. In such a leaky waveguide total internal reflection occurs only at the upper interface beyond the critical angle. We check our findings against experimental data obtained over a concrete pavement overlying an oxisoil.

Numerical Results

In this section we calculate TE-mode dispersion curves that give phase velocity as a function of frequency, or the phase velocity spectrum. Our model is a concrete slab of thickness e and permittivity ε_1, over a substratum of permittivity $\varepsilon_2 > \varepsilon_1$ and $\sigma_2 > \sigma_1$.

A dispersion curve is obtained picking the maxima from the phase velocity spectrum (Park et al., 1998). The thickness e and permittivity ε_1 of the waveguide can be estimated through inversion of the dispersion curve, for a given value of ε_2. A high number of starting models is generated and local minima are investigated in order to obtain a global minimum.

The theoretical dispersion curves are given by (van der Kruk et al., 2006)

$$v(f, \varepsilon_1, e) = c / \sqrt{\varepsilon_1 \sin^2(\theta, \varepsilon_1, e)} \qquad (1)$$

where θ is the angle of incidence on the lower boundary and c is the velocity of light in vacuum. This equation will have solution for θ beyond critical angle and, as it depends on frequency, above a cutoff frequency. Waveguide parameters ε_1, and e are obtained by inverting the picked dispersion curves by minimizing the cost function for each value of ε_2 (van der Kruk ,2006, van der Kruk et al., 2006).

$$\Psi(\varepsilon_1, e) = \frac{1}{n}\sum_{i=1}^{n} \left| v_{picked}(f) - v_{model}(f, \varepsilon_1, e) \right| \qquad (2)$$

Let be the synthetic model with ε_1 = 11, ε_2 =20 and e = 0.2 m. The input Ricker source wavelet has a center frequency of 100 MHz. Figure 1 shows the dispersion curve and the minimum of the penalty function.

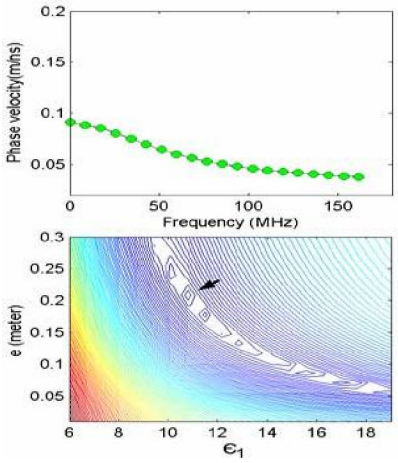

Figure 1. Theoretical dispersion curve for the model ε_1 = 11, ε_2 =20 and e = 0.2 m and the minimum of the penalty function (arrowed in bottom panel).

Experimental Results

Broadside perpendicular CMP and fixed-offset (TE) data were collected on an abandoned factory ground in the City of Manaus. Data were collected over a concrete floor using a Sensors & Software GPR with 100 MHz antennae, 800 ps sampling rate and 32 stack. The spatial intervals were 0.1 m for the CMP data and 0.2 m for the fixed-offset data. We concentrate here in one fixed-offset and two CMP profiles, signaled as R, C1 and C2, respectively in Figure 2.

The concrete floor has two thicknesses e_1 = 0.1 m and e_2 = 0.16 m, as shown in Figure 2, overlaying an oxisol ("Latossolo Amarelo", in Portuguese) engineered into a sizeable flat plateau where the main factory building once stood. Now it remains in place just the concrete floor and several 0.36 m high prismatic concrete supports that once served as base for the roof pillars. The free surface of the two concrete floors is not flush.

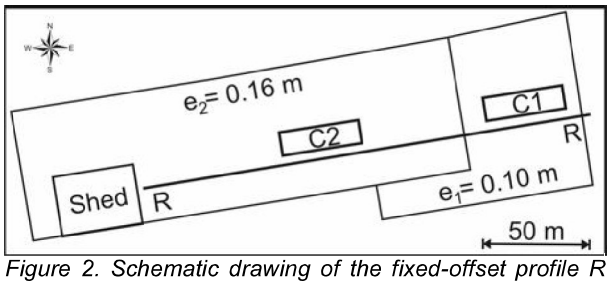

Figure 2. Schematic drawing of the fixed-offset profile R and two CMP profiles, C1 and C2, done on a concrete floor with two thicknesses e_1 = 0.1 m and e_2 = 0.16 m. Profile R begins right beside a storage shed.

The fixed-offset profile R yielded a section with clear indication of tunneling within the thicker concrete. The tunneling appears as phase inversions and as a tuning of the spectrum to a narrow frequency band, as seen in Figure 3. The effect of phase inversions is to broaden the early time apparent wavelet giving an appearance of a conspicuous thick shallow reflector over the thick concrete (Figure 3). The thick concrete waveguide tunes the trace spectrum to a center frequency of F_c = 46.0 ± 0.3 MHz, with a half-width of Δf_h = 26.7 ± 0.7 MHz. In contrast the thinner concrete where the waveguide effect is less prominent the trace spectrum is broader with F_c = 98.6 ± 1.3 MHz and Δf_h = 72.4 ± 2.7 MHz.

We can use F-K filtering to isolate the events in the CMP sections linked to the propagation of superficial waves. The next step is to mute the air wave. Figure 4 shows that C2 conspicuously displays dispersion characteristics. C2 data is used to calculate the phase velocity spectrum shown in Figure 5. We then picked the dispersion curve seen in the same figure. The picked curve is then used in the inversion procedure using 800 starting models.

The value of the refraction index for the soil below the concrete was estimated from a CMP outside the concrete as ε_2 = 20. We have used two values: ε_2 = 15, 20. For the concrete floor we have generated models with 20 x 20 combinations of the refraction index ε_1 and thickness e_2 as in the table below.

Parameter	Min	Max	Step
ε_1	6	19	0.65
e_2 (m)	0.05	0.3	0.0125

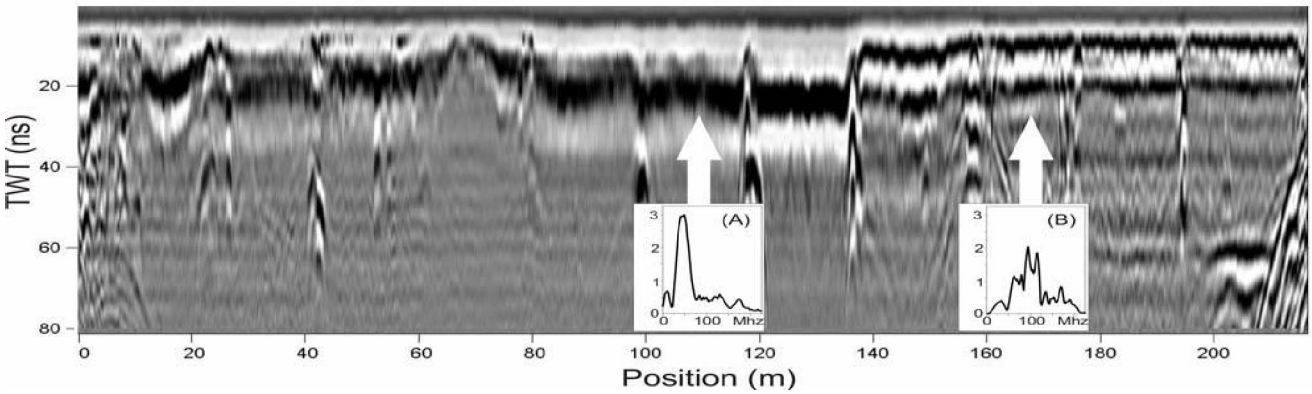

Figure 3. Fixed-offset profile R displaying phase inversions at positions less than 140 m. (A) is the spectrum of the mean of 10 traces located between the two diffractions nearby. (B) is the corresponding spectrum of the 10 traces around the arrowed position. Amplitude units are arbitrary. Each of the several diffractions is due to prismatic concrete supports mentioned in the text.

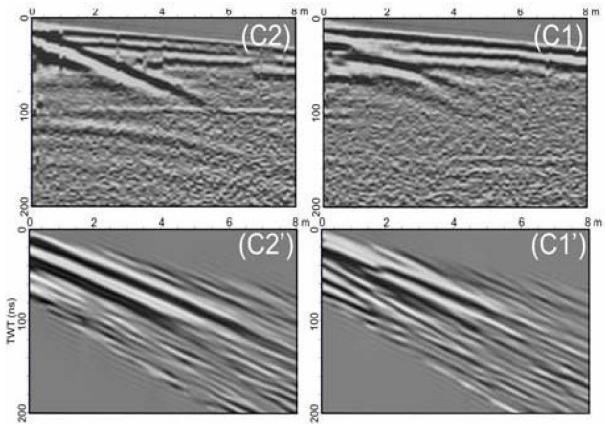

Figure 4. CMP C1 (right panels) and C2 (left panels) before (upper panels) and after F-K filtering. C2 shows clear dispersion characteristics.

The ε_2 = 15 and 20 yielded virtually the same results. The resultant local minima of the penalty function for ε_2 = 20 are plotted in Figure 5. A minimum was found for ε_1 = 11 and e_2 = 0.2 m, values that agree well with the observed thickness (0.16 m) and with the expected value for a humid concrete; local humidity is consistently very high. The dispersion curve and numerical data closely resemble each other. The derived thickness of the waveguide agrees well with the thickness of the concrete and the estimated permittivity fall within the expected range.

Conclusions

GPR wave dispersion can be observed for a two-layer earth model for which the upper layer is a concrete floor with a lower permittivity than the underlining soil. A dispersion curve picked from the phase velocity spectrum and an inversion procedure based on a local minimization algorithm successfully estimated the material properties, which are consistent with information provided by field observations.

Acknowledgements

We thanks Petrobras for supporting this work. LP is a recipient of a DTI/MCT scholarship and JT a CNPq scholarship.

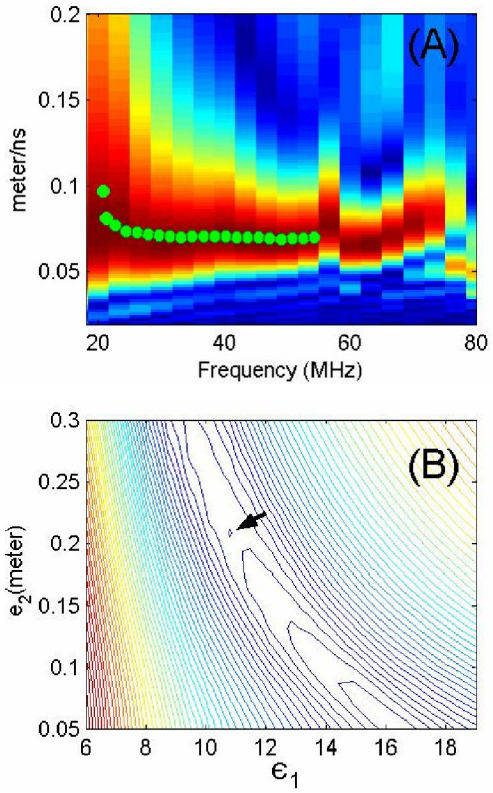

Figure 5. (A) Phase velocity spectrum and picked dispersion curve for the fundamental mode. (B) Penalty function for ε_2 = 20, showing a minimum at ε_1 = 11 and e_2 = 0.2 m.

References

Annan, A. P., W. M. Waller, D. W. Strangway, J. R. Rossiter, J. D. Redman, and R. D. Watts, 1975. The electromagnetic response of a low-loss two-layer dielectric earth for horizontal electric dipole excitation, Geophysics, 40, 285–298.

van der Kruk, J., Arcone, S. A., and Liu, L., 2007, Fundamental and Higher Mode Inversion of Dispersed GPR Waves Propagating in an Ice Layer, IEEE Transactions on Geosciences and Remote Sensing, 45, NO. 8, 2483-2491.

Park, C. B., Miller, R. D. and Xia, J., 1998, Imaging dispersion curves of surface waves on multi-channel record: 68th Annual International Meeting, Society Exploration Geophysicists, Expanded Abstracts, 1377-1380.

Arcone, S . A., Peapples, P. R. and Liu, L., 2003, Propagation of a ground penetrating radar (GPR) pulse in a thin-surface waveguide, Geophysics, 68, 1922–1933.

van der Kruk, J., R. Streich, R., and Green, A. G.,2006, Properties of surface waveguides derived from separate and joint inversion of dispersive TE and TM GPR data, Geophysics, 71, no. 1, K19–K29.

van der Kruk, J., 2006, Properties of surface waveguides derived from inversion of fundamental and higher mode dispersive GPR data, IEEE Transactions on Geosciences and Remote Sensing, 44, no. 10, 2908–2915.